

LETTER TO THE EDITOR

Direct observation of temperature-dependent Fermi surface nesting vectors in a quasi-one-dimensional conductor

A V Fedorov[†], S A Brazovskii[¶], V N Muthukumar[†], P D Johnson[†], J Xue[‡],
L-C Duda[‡], K E Smith[‡], W H McCarroll[§], M Greenblatt[§] and S L Hulbert^{||}

[†] Department of Physics, Brookhaven National Laboratory, Upton, NY 11973-5000, USA

[‡] Department of Physics, Boston University, 590 Commonwealth Avenue, Boston, MA 02215, USA

[§] Department of Chemistry, Rutgers University, Piscataway, NJ 08854-8087, USA

^{||} National Synchrotron Light Source, Brookhaven National Laboratory, Upton, NY 11973, USA

Received 25 January 2000

Abstract. We present the first direct observation of temperature-dependent Fermi wave vectors in the quasi-one-dimensional conductor $K_{0.3}MoO_3$. By monitoring the position of these vectors through the Peierls transition using angle-resolved photoemission spectroscopy, we demonstrate that the temperature dependence of the charge-density-wave vector observed in earlier experiments is actually that of the Fermi wave vectors.

Low-dimensional materials exhibit a number of unique properties closely related to the anisotropy of their Fermi surfaces. Of particular interest are the phase transitions to the state characterized by a charge-density-wave (CDW) instability [1–4]. Much attention has been paid to a class of quasi-one-dimensional (1D) oxides known as blue bronzes with the generic chemical form $A_{0.3}MoO_3$ ($A = K, Rb, \text{ or } Tl$). These compounds possess a highly anisotropic, layered crystal structure. Sheets of corner- and edge-sharing MoO_6 octahedra extend along the 1D direction b , parallel to the $(20\bar{1})$ cleavage plane. These sheets are separated by the ‘A’ cations. The prototypical blue bronze is $K_{0.3}MoO_3$. This material has a metal–semiconductor transition at around 180 K, identified as a Peierls transition, which results in the formation of a gap at the Fermi surface [5]. Electronic structure calculations indicate that two separate quasi-1D bands cross the Fermi level (E_F) in $K_{0.3}MoO_3$.

When a CDW instability occurs in a system that has more than one band crossing E_F , there are two distinct possibilities. One is exemplified by $NbSe_3$ [1] where the system shows two successive transitions with the formation of different CDWs. The other possibility occurs in $K_{0.3}MoO_3$ [3] where diffraction studies clearly reveal just one single CDW with wave vector along the b -direction [6–8]. In the latter case, the CDW wave vector, q_{CDW} , is also found to be temperature dependent. At higher temperatures it is incommensurate with the lattice, and at ~ 100 K it approaches the value expected for a commensurate phase, i.e. $\sim 0.75b^*$ ($b^* = 2\pi/b$ is the reciprocal-lattice unit corresponding to the chain direction). This value of q_{CDW} can be related directly to the Fermi surface nesting vectors given by band-structure calculations: these predict two Fermi wave vectors, $k_{F1} = 0.33b^* = 0.274 \text{ \AA}^{-1}$ and $k_{F2} = 0.42b^* = 0.349 \text{ \AA}^{-1}$, yielding a nesting vector $(k_{F1} + k_{F2}) = 0.75b^* = 0.6234 \text{ \AA}^{-1}$ [9]. Several mechanisms for

[¶] Permanent address: CNRS, Université Paris-Sud, 91406, Orsay Cédex, France.

⁺ Present address: Department of Physics, Uppsala University, Uppsala, S-751 21, Sweden.

the temperature dependence of q_{CDW} have been proposed [7, 10, 11] but to date there has been no experimental evidence that distinguishes between the models. Specifically, there are two distinct possibilities:

- (i) $q_{CDW}(T)$ follows a hidden dependence of $(k_{F1} + k_{F2})(T)$;
- (ii) $q_{CDW}(T)$ deviates from $(k_{F1} + k_{F2})$ due to phonon dispersion or due to a breaking of the charge-conjugation symmetry.

In principle, angle-resolved photoemission spectroscopy (ARP) is an experimental probe that can be used to distinguish between these two models, since it can be used to measure the Fermi wave vectors directly. Early ARP work on $K_{0.3}MoO_3$ performed at 300 K reported only one band crossing the Fermi level at $k_F \simeq 0.312 \text{ \AA}^{-1}$ [12], while a more detailed study revealed the existence of two bands [13] in the vicinity of E_F , in agreement with theory [9]. However, there have been no reports of ARP studies of the temperature dependence of these Fermi wave vectors. In view of the temperature dependence of q_{CDW} found in x-ray and neutron scattering, the availability of such data would help in our understanding of CDWs in the blue bronzes and other quasi-1D materials. To be successful, such a study requires a considerable improvement in the momentum resolution of ARP in order to bring it to the same level as that obtained routinely in x-ray and neutron scattering experiments.

We report here the first direct observation of temperature-dependent Fermi wave vectors in $K_{0.3}MoO_3$. We identify two parallel bands dispersing along the chain direction ΓX towards E_F and crossing at momentum values k_{F1} and k_{F2} (see figure 1). We find that the Fermi wave vectors are temperature dependent and that the temperature dependence of the sum $(k_{F1} + k_{F2})$ is identical to that of q_{CDW} found in x-ray and neutron studies. Our results show unambiguously that the temperature dependence of the nesting wave vector is due to that of the Fermi wave vectors, thereby providing strong constraints on any theoretical description.

The photoemission experiments were performed with a hemispherical electron energy analyser SES-200 (Scienta) using photons from the U13UB beamline at the National Synchrotron Light Source. The photon energy used in this study was 21.4 eV. The total energy resolution obtained was ~ 15 meV, while the momentum resolution was better than 0.01 \AA^{-1} . Single crystals of $K_{0.3}MoO_3$ were grown by using the gradient flux technique [14]. They were mounted on an open-cycle He refrigerator. By changing the rate of He flow, we were able to stabilize sample temperatures between 15 K and 300 K with an accuracy of ± 1 K. Clean stoichiometric surfaces of $K_{0.3}MoO_3$ were prepared by cleaving samples along the (201) plane *in situ*. Sample alignment was verified by means of low-energy electron diffraction which showed sharp spots with virtually no diffuse background. The base pressure in the chamber was below 3×10^{-11} Torr. The spectrometer is capable of multi-channel data collection such that the output signal is a three-dimensional map with the X- and Y-axes corresponding to the emission angle and the kinetic energy of photoelectrons respectively. The Z-axis is the raw photocurrent intensity at each XY-point.

Figure 1(a) displays a typical ARP map of the electronic structure of $K_{0.3}MoO_3$ in the region close to the Fermi level crossings. This is a full, essentially continuous, three-dimensional map of the photocurrent in this region of energy and momentum space—this is in contrast to photointensity maps generated for one value of energy (usually E_F), where intensity is recorded at discrete points in angle space by physically moving either the analyser or the sample. To extract conventional energy distribution curves (EDCs) from figure 1(a), one simply cuts the intensity map at the desired point along the x-axis, i.e. at the desired value of the momentum. However, a plot such as figure 1(a) is more useful than conventional EDCs since it also shows the variation of the photocurrent with momentum at any particular energy. The experimental data reveal the existence of two bands that are parallel in the vicinity of the

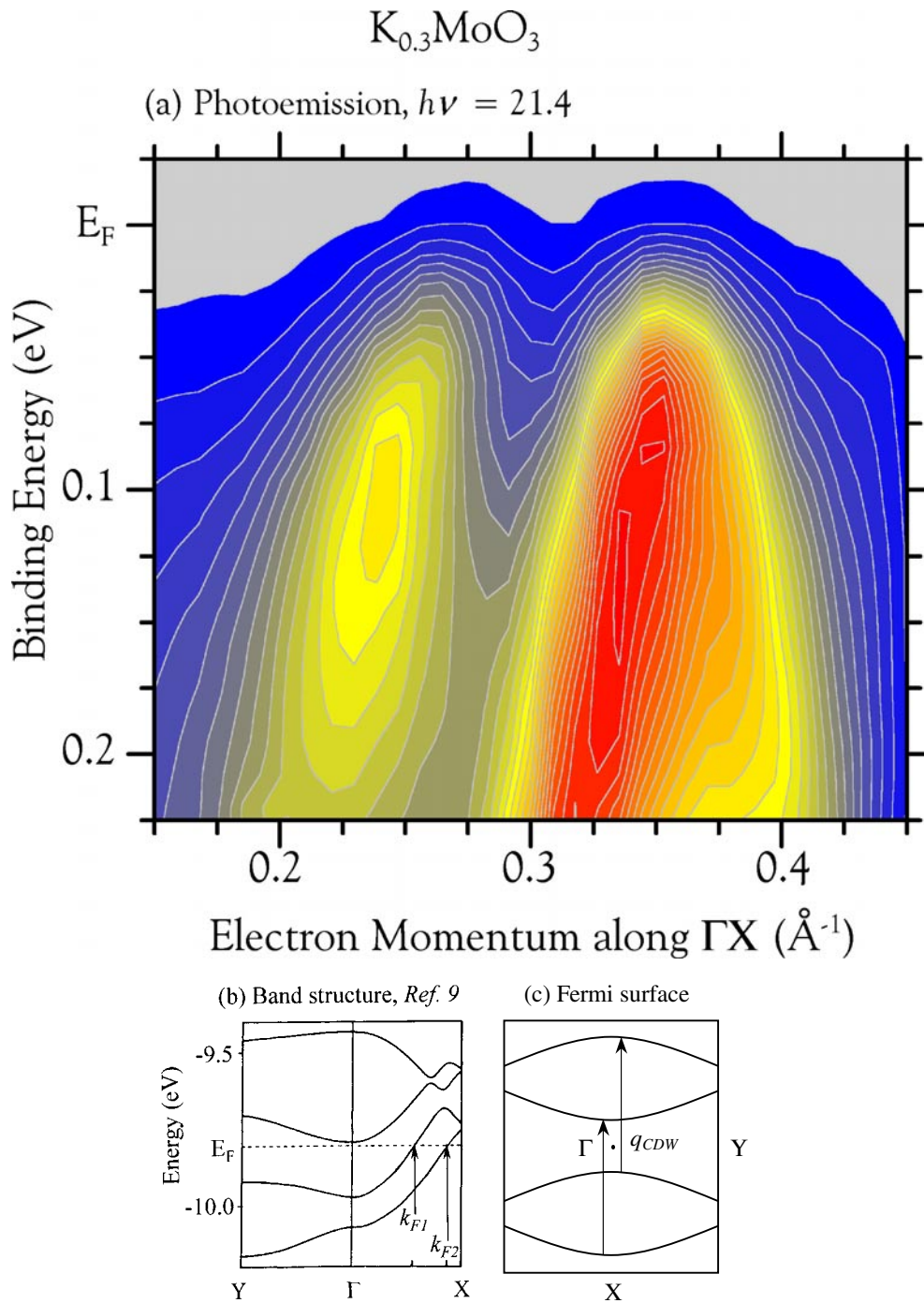


Figure 1. (a) A photoemission intensity map of $\text{K}_{0.3}\text{MoO}_3$; intensity increases from blue to red; (b) the band structure of $\text{K}_{0.3}\text{MoO}_3$ from reference [9]; (c) a schematic sketch of the Fermi surface (for details see the text).

Fermi level and split by ~ 480 meV. Figure 1(b) shows the results of a tight-binding band-structure calculation [9] and the experimentally observed emission features in figure 1(a) are clearly related to the bands found in the calculation, indicating that they are formed by the d bands of Mo. The calculated splitting of 160 meV is, however, three times smaller than that found experimentally. In figure 1(c), we show a schematic Fermi surface. It is composed of two lines of opposite curvature, suggesting that the lower Fermi surface of the first band is nested in the upper Fermi surface of the second band and vice versa [7, 9]. Consequently, the single CDW observed in x-ray and neutron scattering experiments has a wave vector which equals the sum of the two Fermi wave vectors, $(k_{F1} + k_{F2})$. These wave vectors can now be determined with high precision using the data of figure 1(a).

In general, there are two ways of using ARP to measure Fermi wave vectors. The first involves measuring a series of EDCs, and tracking the dispersion of an emission feature as it crosses above E_F . This is quite sufficient for simple systems, but becomes problematic for complex conductors since knowledge of model spectral functions is required, which is an area of intense theoretical discussion [15]. Alternatively, one can measure the intensity of photoelectrons versus momentum at E_F . Such a method was in fact successfully used for measuring the Fermi surface in the normal state of the high-temperature superconductor $\text{Bi}_2\text{Sr}_2\text{CaCu}_2\text{O}_8$ [16] and more recently for the demonstration of the absence of well-defined quasiparticle excitations in the same material [17]. Exploiting the natural capabilities of our spectrometer, we use the latter method. The procedure simply consists of taking intensity versus momentum profiles at E_F from the ARP map in figure 1(a) and identifying the points of highest intensity. We recently reported the use of this technique to successfully measure the Fermi surface in another quasi-1D system [18].

Figure 2 shows the photoemission intensity at E_F as a function of sample temperature and momentum. This set of constant-energy profiles was obtained by integrating the temperature-dependent 3D ARP maps in an energy window of $E_F \pm 5$ meV. Each profile consists of two well-defined peaks, corresponding to the two bands crossing E_F , from which k_{F1} and k_{F2} can be immediately identified. To verify that they do correspond to Fermi level crossings, we produced a traditional energy distribution curve (EDC) by cutting the photocurrent map in an angular window of 0.2° centred at angle corresponding to k_{F2} . The result is shown as an inset in figure 2. The solid line through the data points is a Fermi edge of the Au film deposited on the sample. We clearly observe significant intensity at E_F , and an unambiguous Fermi cut-off. This is in sharp contrast to earlier reports [13] based on the use of an electron spectrometer with conventional, i.e. $\pm 1^\circ$, angular resolution. (Significantly, we found that cutting the intensity map at slightly different angles or using a window of 2° results in EDCs with intensity greatly suppressed at E_F .) When the temperature is lowered below 180 K, the intensity of both peaks gradually decreases, reflecting the gap opening at E_F associated with the Peierls transition. The data reveal that the gap does not open fully, and there is enough intensity at E_F for us to track the position of the Fermi wave vector(s) through the Peierls transition. This could either be due to fluctuations of the CDW order parameter [4] or the formation of amplitude solitons [19]. However, the data of figure 2 also show that there is a reduction of the *splitting* between the peaks, implying an increase of $(k_{F1} + k_{F2})$ for temperatures between 180 K and 100 K. This increase is dominated by the movement of k_{F1} towards k_{F2} . While the former exhibits a strong temperature dependence, the latter does not appear to show any systematic shift with temperature, but we cannot exclude a slight temperature dependence of k_{F2} beyond our momentum resolution.

For a more quantitative analysis, the constant-energy profiles were fitted using a least-squares procedure to two Gaussians representing peaks at k_{F1} and k_{F2} , respectively. A linear background was superimposed to account for scattered electrons. The intrinsic widths of the

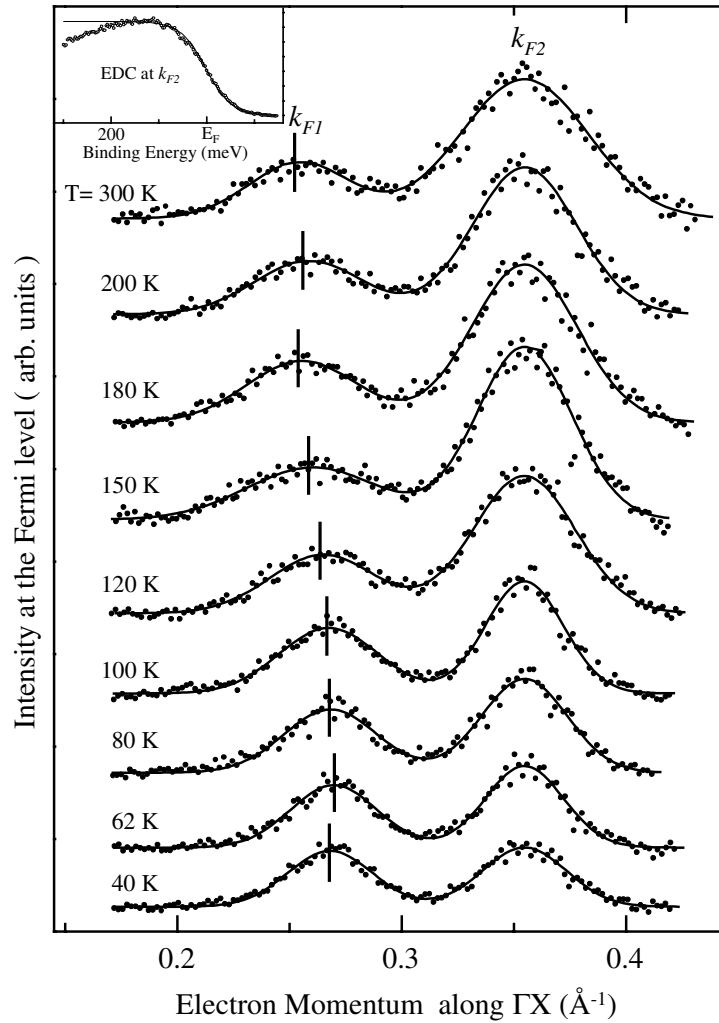


Figure 2. Results of the least-squares-fit analysis of intensity versus electron momentum profiles at the Fermi level. The inset shows the EDC measured at the emission angle corresponding to the Fermi wave vector k_{F2} . The solid line represents the experimentally determined Fermi edge measured from an evaporated gold film.

Gaussians were found to decrease slightly upon cooling the sample. The solid line through the data points in figure 2 represents the results of the fit. The value of $[1 - (k_{F1} + k_{F2})]$ determined in this manner is plotted versus temperature in figure 3. On the same figure, we have also shown the temperature dependence of the reduced wave vector of the CDW, $(1 - q_{CDW})$, obtained from the inelastic neutron scattering [8]. The two curves coincide well, showing that the temperature dependence of the nesting wave vector is due to that of the Fermi wave vector. We now consider the implications of this result.

It was suggested earlier by Pouget *et al* that there exists a flat band just above E_F in $K_{0.3}MoO_3$ which can be thermally populated [7]. The temperature dependence of q_{CDW} can then be attributed to charge transfer between the two bands crossing E_F and the third band. Such an explanation can also account for a temperature-dependent k_F . (Band-structure calculations

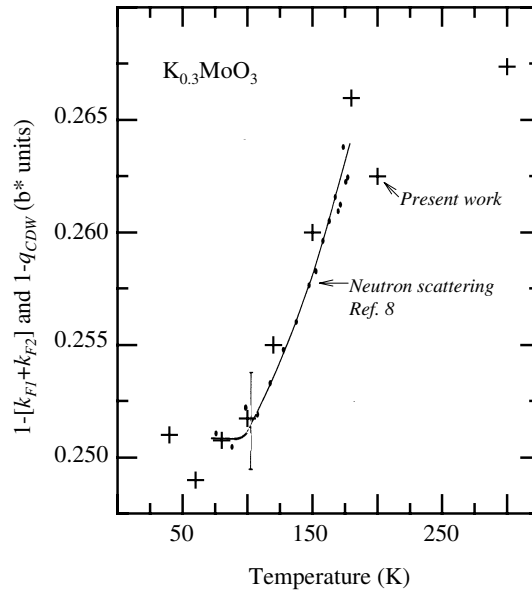


Figure 3. The temperature dependence of $[1 - (k_{F1} + k_{F2})]$ derived from the data in figure 2 (crosses) and the temperature dependence of $(1 - q_{CDW})$ measured by means of neutron scattering in reference [8].

do indeed show a third band located at 0.012 eV above E_F at Γ , but it disperses rapidly to higher energies away from the zone centre [9].) However, a natural consequence of this would be a continuous change in k_F between 180 K and 300 K. Our results, on the other hand, indicate that k_F begins to saturate at higher temperatures, thereby ruling out a simple charge-transfer model. There have also been explanations for the temperature dependence of the nesting wave vector. Noguera and Pouget [10] have shown that a nonlinear electron dispersion as well as a finite phonon dispersion can lead to the thermal dependence of the nesting wave vector. Artemenko *et al* [11] have also proposed a similar explanation but differing in detail. In both of these models, the thermal dependence of the nesting wave vector follows from a shift in the chemical potential. However, such models cannot explain our results for the temperature dependence of the Fermi wave vectors that we obtained at a *constant* energy E_F . The absence of any detectable shift of the bands at high binding energies is also not consistent with a shift in the chemical potential. Indeed, the ARP data show that the temperature dependence of the nesting wave vector in $K_{0.3}MoO_3$ is predominantly (if not completely) due to a change in the electronic structure.

Since the change in the Fermi wave vectors of $K_{0.3}MoO_3$ occurs between 100 K and 200 K, it is reasonable to associate any change in the electronic structure with a change in the coupling between chains belonging to different unit cells (the smallest electronic scale in the problem). This can happen if, for instance, the Mo–O distances in the basal plane change continuously with temperature. To explore this possibility, we have calculated the Fermi surface using a tight-binding model. The model Hamiltonian represents an array of coupled chains with two chains per unit cell. The coupling between these two chains, t_{\perp} , is chosen to be 0.3 (in units of the intrachain hopping integral t). The coupling t'_{\perp} between adjacent chains belonging to different unit cells is chosen to be 0.1 in the same units. If we change t'_{\perp} in our tight-binding model by 10%, we find that the splitting between the Fermi wave vectors along the 1D direction

$k_{\perp} = 0$ changes by 5%. The result of such a calculation is shown in figure 4 with full and dashed lines representing, respectively, the initial Fermi surface and that corresponding to the t'_{\perp} reduced by 10%. Experimentally, the splitting reduces by 10% as the temperature is lowered. For a given number of electrons, this would also imply a change in the Fermi wave vector transverse to this direction. Hence, the CDW nesting vector should also change along the transverse direction. This and related consequences are being currently investigated.

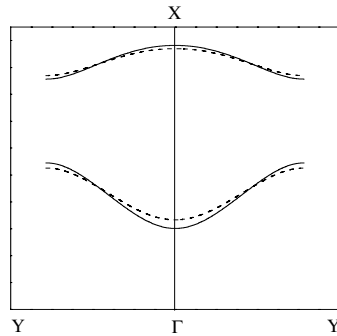


Figure 4. The Fermi surface of an array of coupled chains with two chains per unit cell calculated using a tight-binding model (solid lines). Reducing the interchain splitting by 10% leads to the Fermi surface indicated by the dashed lines.

To summarize, using ARP with high momentum resolution we have directly measured two Fermi wave vectors in quasi-one-dimensional $K_{0.3}MoO_3$. By monitoring the temperature dependence of the Fermi wave vectors from 300 to 40 K, it was possible for the first time to compare the temperature dependence of the Fermi wave vectors and the CDW nesting vector. Our results show unambiguously that the temperature dependence of the CDW nesting vector observed in x-ray and neutron scattering experiments is primarily due to a change in the electronic structure.

Work at BNL is supported in part by DE-AC02-98CH10886. The Boston University programme is supported in part by the Department of Energy under DE-FG02-98ER45680. Research was undertaken at the NSLS, which is supported by the US DOE, Divisions of Materials and Chemical Sciences.

References

- [1] Monceau P 1985 *Electronic Properties of Inorganic Quasi-One-Dimensional Compounds (Physics and Chemistry of Materials with Low-Dimensional Structures, Series B: Quasi-One-Dimensional Structures)* ed P Monceau (Dordrecht: Reidel)
- [2] Rouxel J (ed) 1986 *Crystal Chemistry and Properties of Materials with Quasi-One-Dimensional Structures* (Dordrecht: Reidel)
- [3] Dumas J and Schlenker C 1993 *Int. J. Mod. Phys. B* **7** 4045
- [4] Grüner G 1994 *Density Waves in Solids (Frontiers in Physics vol 89)* (Reading, MA: Addison-Wesley)
- [5] Travaglini G *et al* 1981 *Solid State Commun.* **37** 599
- [6] Sato M, Fujishita H and Hoshino S 1983 *J. Phys. C: Solid State Phys.* **16** L877
- [7] Pouget J P *et al* 1985 *J. Physique* **46** 1731
- [8] Flemming R M, Schneemeyer L F and Moncton D E 1985 *Phys. Rev. B* **31** 899
- [9] Whangbo M-H and Schneemeyer L F 1986 *Inorg. Chem.* **25** 2424
- [10] Noguera C and Pouget J P 1991 *J. Physique I* **1** 1035
- [11] Artemenko S N, Pokrovskii V Ya and Zaitsev-Zotov S V 1996 *Sov. Phys.-JETP* **83** 590

- [12] Veuillen J V, Cinti R C and Al Khoury Neme E 1987 *Europhys. Lett.* **3** 355
- [13] Gweon G-H *et al* 1996 *J. Phys.: Condens. Matter* **8** 9923
- [14] Ramanujachary K V, Greenblatt M and McCarroll W H 1984 *J. Cryst. Growth* **70** 476
- [15] Meden V and Schönhammer K 1992 *Phys. Rev. B* **46** 15 753
Voit J 1993 *J. Phys.: Condens. Matter* **5** 8305
Ren Yong and Anderson P W 1993 *Phys. Rev. B* **48** 16 662
- [16] Aebi P *et al* 1994 *Phys. Rev. Lett.* **72** 2757
- [17] Valla T *et al* 1999 *Science* **285** 2110
- [18] Xue J *et al* 1999 *Phys. Rev. Lett.* **83** 1235
- [19] Brazovskii S A 1980 *Sov. Phys.-JETP* **51** 342